Morphologies resulting from the directional propagation of fractures

L. Pauchard,[1,*] M. Adda-Bedia,[2] C. Allain[1] and Y. Couder[2]
[1]*FAST, Bâtiment 502, Campus Universitaire d'Orsay, 91405 Orsay Cedex, France*
[2]*Laboratoire de Physique Statistique, École Normale Supérieure, 24 Rue Lhomond, 75231 Paris Cedex 05, France*
(Received 3 July 2002; revised manuscript received 13 December 2002; published 26 February 2003)

When growing in a stress gradient, cracks have a directional growth. We investigate here this type of instability in the case of a colloidal gel deposited on a substrate and left to dry. The use of various materials reveals the existence of two distinct types of dynamics. When the crack nucleation is easy a well known situation is reached: an array of periodic fractures forms, which grow parallel to each other and move quasistatically with the stressed region. In contrast, in materials where the crack nucleation is difficult, a subcritical process is observed with the retarded formation of isolated cracks which move faster and which display an arch shaped trajectory. This type of process appears to be generic in all cases where there is delayed nucleation. This is confirmed by experiments on the directional propagation of cracks in thermally stressed glass.

DOI: 10.1103/PhysRevE.67.027103 PACS number(s): 62.20.Mk, 47.54.+r, 81.40.Np, 82.70.Dd

Many morphological instabilities due to growth in opened media can be obtained in different experimental configurations where the relevant field has an imposed moving spatial variation. These are usually called directional instabilities. For instance, the directional growth of crystals occurs in an imposed moving temperature gradient [1,2] and directional viscous fingering in an imposed pressure gradient [3,4]. Similarly, if a strong stress gradient (induced by a given diffusion field) is created in a material, a regime of directional growth of cracks can be observed. This directional growth has been investigated in glass plates submitted to a thermal gradient [5–8] and in the drying of a colloidal gel enclosed in a thin cell [9,10]. In both experiments, if the sample is wide, an array of parallel cracks is formed. These quasistatic fractures propagating at the low velocities imposed by the moving gradient have been studied theoretically [11,12]. Here, we study the fractures induced by the drying of a concentrated suspension of colloidal particles simply deposited on a glass plate. Depending on the system studied, different patterns are observed. Thus, in a colloidal gel of latex particles (diameter$\cong 0.1\ \mu$m), the usual evolution of a regular array of straight parallel cracks is observed [Fig. 1(a)]. On the contrary, during the drying of a concentrated colloidal suspension of nanolatex particles in water (diameter$\cong 0.02\ \mu$m), different patterns are observed. As seen in Fig. 1(b), the cracks form a mesh of arches whose symmetry axes are approximately perpendicular to the drying front. Such a pattern has, to our knowledge, only been described once in the desiccation of thin layers of an alumina-water slurry [13]. In the following, we characterize both the dynamics of a single arch shaped crack and that of the mesh they form.

In the experiments, a small quantity of suspension is deposited on a horizontal glass plate and then spread so as to form a layer having a slight thickness gradient in the X direction. The layer is left to desiccate by evaporation at room temperature and fixed humidity rate; a process which, under our experimental conditions, is limited by diffusion of water into air. As usual for colloidal suspensions, the substrate–air–colloidal-suspension contact line, i.e., the three-phase contact line, is strongly anchored on the glass slide, so that the surface of contact between the layer and the substrate remains constant during drying [14–16]. Because of water loss, particles and ionic species accumulate. When the particle volume fraction reaches a threshold value (fixed by the physicochemical conditions) the suspension gels. Since drying is faster in the thinner region (smaller water volume for a given area) a front is formed which separates the region where the suspension is gelled from that where the suspension is still fluid. Under the microscope, this gelation front, observed as a line between two different refractive media, propagates in the direction of the thickness gradient. The gel keeps drying and tends to shrink but is prevented from doing so by the adhesion on the substrate. This growing mismatch results in stresses increasing with time until they reach a value large enough to nucleate and then propagate cracks.

In the case of latex particles [Fig. 1(a)] the cracks propagate along the X direction, closely following the drying front and moving at the same velocity. The pattern is a periodic array of parallel fractures with a wavelength related to the local thickness of the sample. So, as the thickness increases

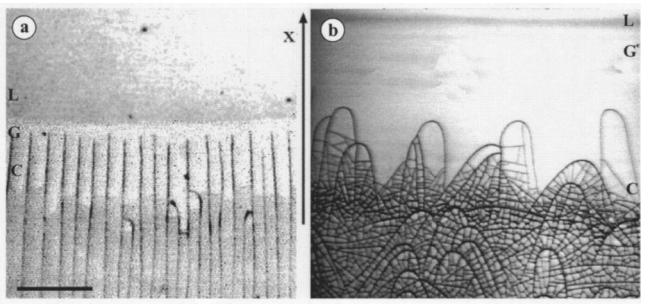

FIG. 1. Photographs of the directional growth of fractures (the scale is given by the bar$=200\ \mu$m) in the drying of a suspension of (a) latex particles and (b) nanolatex particles. On each photograph (L) is the region where the solution is still liquid, (G) the region where it has become a gel, and (C) the region where the gel is fractured.

*Author to whom correspondence should be addressed. Email address: pauchard@fast.u-psud.fr

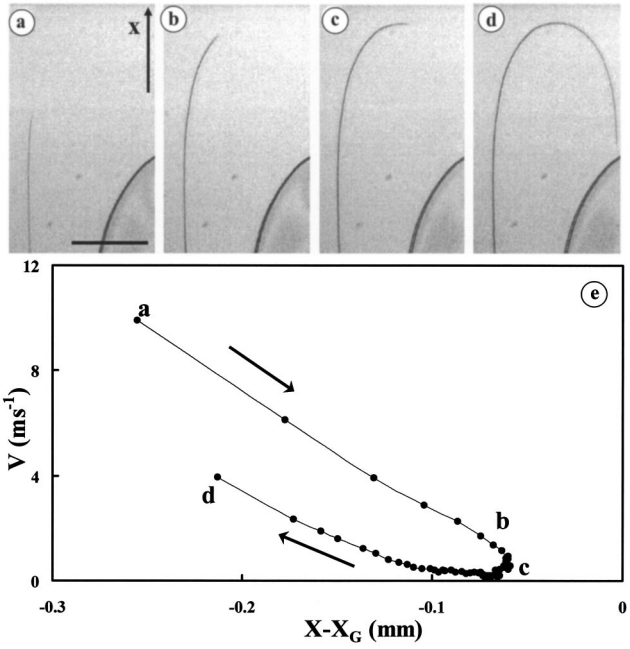

FIG. 2. Successive images (a), (b), (c), (d) taken at time intervals of 4×10^{-3} s, showing the propagation of a single arch shaped fracture (bar=50 μm). (e) Norm of the crack velocity V as a function of $|X-X_G|$, the instantaneous distance of its tip from the gelation front.

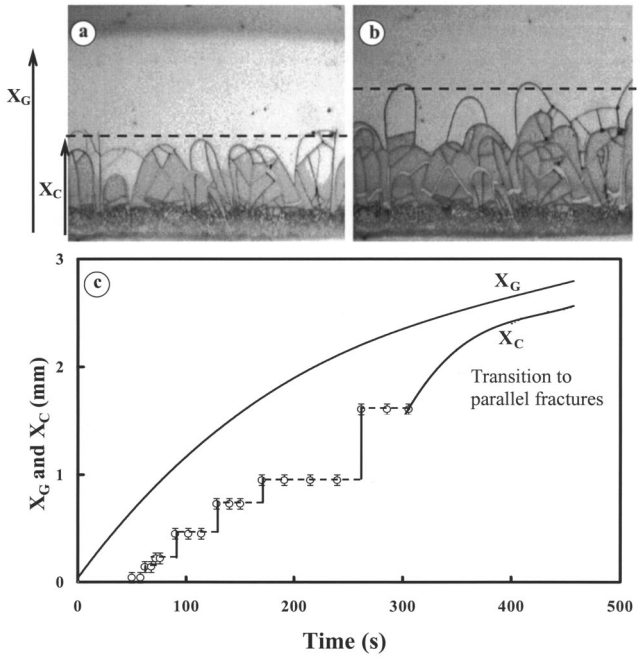

FIG. 3. Time evolution of the position of the gelation front X_G and of the envelope of the cracks X_C in the experiment performed with nanolatex particles.

along the X axis, readjustments of the periodicity occur: some cracks stop growing by connecting perpendicularly to one of their neighbors [Fig. 1(a)]. More generally, the final spacing between cracks, λ, increases linearly with the layer thickness h, with a prefactor depending on several related physical parameters: the gel thickness [9,17–19], physicochemical properties [20], adhesion of the gel onto the substrate [13,19], and desiccation conditions. Later, an interfacial fracture occurs that separates the gel from the substrate. This is a delamination front which follows the cracking front and releases the residual stresses [see Fig. 1(a)].

When the same experiment is repeated with a suspension of nanolatex particles, the observed dynamics is different and results in another morphology [Fig. 1(b)]. A crack now forms in isolation, far behind the drying front, perpendicularly to a previous crack. This initial direction of growth of the crack is usually not aligned with the direction of propagation of the drying front. A given crack propagates fast and follows a curved trajectory. Using a high-speed video camera, we investigated the dynamics of crack propagation. Figures 2(a)–2(d) show a series of images for an arch shaped crack. When the crack tip approaches the drying front, the crack curves and loops back to propagate toward the driest region of the gel. The measurements of the crack tip velocity are presented on Fig. 2(e) as a function of the distance to the drying front. The initial speed (of the order of 4 m s^{-1}) is small compared to the Rayleigh wave speed (estimated to be 100 m s^{-1}) but large compared to the velocity of the drying front (10 μm s^{-1}). As the crack tip approaches the drying front its speed decreases, reaches a nonzero minimum at the apex, and then increases during the return toward the driest region. As soon as a new arch is completed a mesh of narrowly spaced linear cracks forms but only in the region inside the arch [13].

The collective invasion of the gel by the cracks occurs discontinuously. At certain times several arch shaped cracks form practically simultaneously in different regions of the front. Their envelope, which forms a straight line parallel to the gelation front [Fig. 3(a)], advances rapidly during these periods. Two periods of crack formation are separated by a time interval during which the envelope is motionless while the stresses, ahead of it, build up. This is shown in Fig. 3(c) where are plotted the time evolution of X_G, the position of the gelation front, and X_C, the envelope of the cracks (the origin of the X axis being at the three-phase line). While the former moves smoothly the latter exhibits a step by step behavior. As the drying front moves on, cracks propagate in a layer which becomes thicker and a return to the usual crack pattern is observed. In this way the new cracks nucleated from preexisting arch shaped cracks now propagate toward the gelation front and simply follow it [Fig. 3(c)]. An array of regularly spaced parallel fractures propagates quasistatically.

The first difference between the cracks obtained in latex and nanolatex lies in the nucleation process. In the former case many germs of cracks allow for the parallel crack organization; this array of cracks advances quasistatically following the gelation front. In contrast, in nanolatex nucleation is more difficult. As the gelation front propagates, nucleation is delayed; fractures form but only far away from the front. Then they propagate fast in the space that separates them from the gelation front. This suggests that the nucleation of a new crack requires more energy than its propagation so that a subcritical behavior is observed (of the type of the stick-

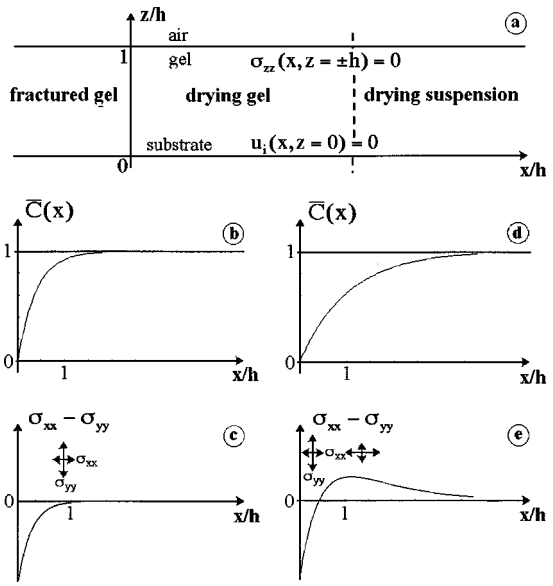

FIG. 4. (a) Scheme of a vertical section of the gel. The boundary conditions are given at the air/gel interface ($z=h$), and on the substrate ($z=0$). The moving O_X axis has its origin ($x=0$) on the crack front. (b) The mean concentration field of solvent $\overline{C}(x) = (1/2h)\int_{-h}^{h} C(x,z)dz$ is given when the two fronts are near each other ($\xi \sim h$). The corresponding stress tensor difference $\sigma_{xx}-\sigma_{yy}$ is shown in (c). (d) The mean concentration field when the fronts are far from each other ($\xi \sim 5$ h). In this case, $\sigma_{xx}-\sigma_{yy}$ shown in (e) changes sign.

slip process in friction). We ascribe this behavior to the better homogeneity of the nanolatex gels. This is confirmed by two other observations. (i) The crack surfaces in latex are irregular while they are smooth in nanolatex. (ii) When some latex particles are added to the nanolatex (a few percent), the medium becomes inhomogeneous: easy nucleation sites are created and the arch shaped cracks do not form.

We can now show that the resulting difference of the distance from the crack front to the gelation front is responsible for the change in crack morphology. With latex particles, the cracks follow the gelation front at a distance of the order of the layer thickness. With nanolatex the cracks form and grow much further away from the gelation front. Let us consider the fracture-free area between the cracking front and the gelation front [using moving coordinates with the origin of the Ox axis on the fracture front, i.e., at X_C as shown in Fig. 3(a)]. In this region, the stress distribution is due to the diffusive concentration field of the solvent. Taking into account the symmetrical image of the region with respect to $z=0$ we introduce an instantaneous reduced solvent concentration field $C(x,z)$, as presented in Fig. 4(b) or 4(d):

$$C(x,z) = C_0(x) + \left(\frac{z}{h}\right)^2 C_1(x). \tag{1}$$

In this problem $C(x,z)$ does not depend on y because of the absence of neighboring cracks [note that $C(x,z)$ is an adimensional quantity varying from 0 for a completely dried gel to 1 for the colloidal suspension]. Assuming that the material is both isotropic and homogeneous and in a state of plane strain, the classical theory of elasticity is applicable. The stress tensor is given by

$$\sigma_{ij} = \frac{E}{1+\nu}\left(u_{ij} + \frac{\nu}{1-2\nu}\delta_{ij}\sum_{1=x,y,z} u_{ll}\right) - \frac{E}{1-2\nu}C(x,z)\delta_{ij}, \tag{2}$$

where E and ν, respectively, denote Young's modulus and the Poisson number, and $u_{ij} = (\partial_i u_j + \partial_j u_i)/2$ holding for $i = x,y,z$ represents the deformation tensor with respect to the displacement fields u_i so that $u_x = (z/h)^2 f(x)$, $u_z = (z/h)\, g(x)$ (f and g being arbitrary functions of x). The equilibrium condition complemented by the boundary conditions [see Fig. 4(a)] allows calculation of the stress distribution in the consolidating region of gel. This leads to the following form for the stress difference $\sigma_{xx}-\sigma_{yy}$:

$$\sigma_{xx}-\sigma_{yy} = E[\beta(h,\nu)e^{-\alpha(\nu)x/h} + \gamma(h,\xi,\nu)e^{-x/\xi}], \tag{3}$$

where ξ is the characteristic length in which the concentration of solvent is established along x; α, β, and γ are functions of h, ξ, ν. Two cases can be distinguished.

(a) When ξ is of the order of the layer thickness h [Fig. 4(b)], the stress difference $|\sigma_{xx}-\sigma_{yy}|$ decreases with increasing distance x from 0 toward the gelation front [Fig. 4(c)]. Since $\sigma_{xx}-\sigma_{yy}$ is always negative σ_{yy} is more efficient than σ_{xx} in inducing fracture opening. As a consequence cracks move in the X direction.

(b) In contrast, when ξ is larger than h [Fig. 4(d)], the stress $|\sigma_{xx}|$ decreases but more slowly than $|\sigma_{yy}|$. This results in a change of sign in $\sigma_{xx}-\sigma_{yy}$ at a certain distance of the crack front [Fig. 4(e)]. Thus σ_{xx} becomes more and more efficient with respect to σ_{xx}. The fracture propagating in this field will thus rotate to keep releasing the main stress, following the Cotterell-Rice principle [21]. When the fracture has reached the apex of the arch its motion is transitorily parallel to Oy. Since the crack usually has no close neighbors, the region that separates it from the previous front is still highly stressed. At this point the crack thus keeps turning so as to return to the drier (and more stressed) region where it will accelerate, releasing the σ_{yy} stress again.

Finally, we reconsidered directional crack propagation [5–8] in glass plates submitted to a thermal gradient. In this homogeneous material the nucleation of a new crack is difficult. In the reported experiments using wide samples [6–8] the growth of parallel cracks was observed. However, in all cases the experimentalists overcame the nucleation problem by artificially creating notches at the sample's border before starting the experiment. We reproduced these experiments without these artificial nuclei. In this situation, fewer cracks form and they propagate fast along arch shaped trajectories. The formation of arches thus appears to be generic in the directional propagation of fractures whenever their formation is retarded by the difficulty of their nucleation.

We thank L. Mahadevan and B. Perrin for useful discussions.

[1] K. A. Jackson and J. D. Hunt, Trans. Metall. Soc. AIME **236**, 1129 (1966).
[2] M. Georgelin and A. Pocheau, Phys. Rev. E **57**, 3189 (1998).
[3] M. Rabaud, S. Michalland, and Y. Couder, Phys. Rev. Lett. **64**, 184 (1990).
[4] H. Z. Cummins, L. Fourtune, and M. Rabaud, Phys. Rev. E **47**, 1727 (1993).
[5] A. Yuse and M. Sano, Nature (London) **362**, 329 (1993).
[6] O. Ronsin, O. Heslot, and B. Perrin, Phys. Rev. Lett. **75**, 2352 (1995).
[7] M. Marder, Phys. Rev. E **49**, R51 (1994).
[8] M. Adda-Bedia and Y. Pomeau, Phys. Rev. E **52**, 4105 (1995).
[9] C. Allain and L. Limat, Phys. Rev. Lett. **74**, 2981 (1995).
[10] T. Boeck, H. A. Bahr, S. Lampenscherf, and U. Bahr, Phys. Rev. E **59**, 1408 (1999).
[11] E. A. Jagla, Phys. Rev. E **65**, 046147 (2002).
[12] S. Kitsunezaki, Phys. Rev. E **60**, 6449 (1999).
[13] K. A. Shorlin, J. R. de Bruyn, M. Graham, and S. W. Morris, Phys. Rev. E **61**, 6950 (2000).
[14] F. Parisse and C. Allain, J. Phys. II **6**, 1111 (1997).
[15] F. Parisse and C. Allain, Langmuir **13**, 3598 (1997).
[16] R. D. Deegan, O. Bakajin, T. F. Dupont, G. Huber, S. R. Nagel, and T. Witten, Nature (London) **389**, 827 (1997).
[17] A. Atkinson and R. M. Guppy, J. Mater. Sci. **26**, 3869 (1991).
[18] H. Colina and S. Roux, Eur. Phys. J. E **1**, 189 (2000).
[19] A. Groisman and E. Kaplan, Europhys. Lett. **25**, 415 (1994).
[20] L. Pauchard, F. Parisse, and C. Allain, Phys. Rev. E **59**, 3737 (1999).
[21] B. Cotterell and J. R. Rice, Int. J. Fract. **16**, 155 (1980). According to Cotterell and Rice, the local stress field at the tip of a slightly curved two-dimensional crack is of a mode I type (opening mode) and the shear mode (mode II) equals zero as the crack extends. Note that if the shear mode is not equal to zero at the crack tip, the crack extends with an abrupt change in the tangent direction to the path (kink).